

Analysis of transcriptome sequencing of sciatic nerves in Sprague-Dawley rats of different ages

Jiang-Hui Liu^{1,*}, Qing Tang^{2,*}, Xiang-Xia Liu², Jian Qi³, Rui-Xi Zeng², Zhao-Wei Zhu^{2,*}, Bo He^{4,*}, Yang-Bin Xu²

1 Department of Emergency, First Affiliated Hospital of Sun Yat-sen University, Guangzhou, Guangdong Province, China

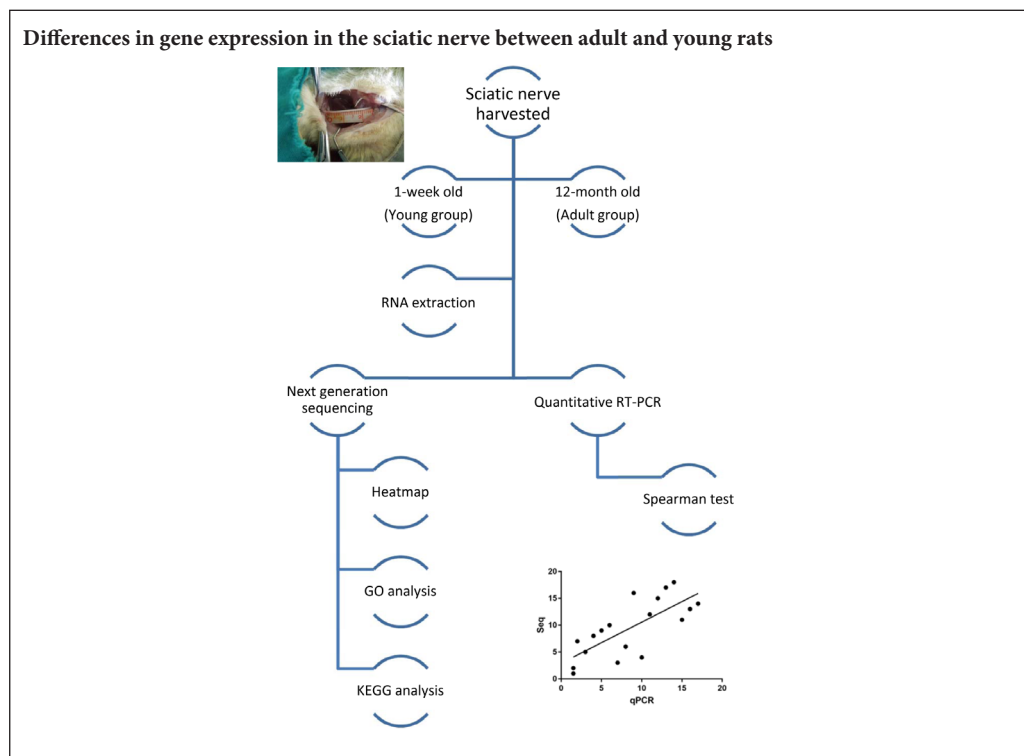
2 Department of Plastic Surgery, First Affiliated Hospital of Sun Yat-sen University, Guangzhou, Guangdong Province, China

3 Department of Orthopedics and Microsurgery, First Affiliated Hospital of Sun Yat-sen University, Guangzhou, Guangdong Province, China

4 Department of Orthopedics, Third Affiliated Hospital of Sun Yat-sen University, Guangzhou, Guangdong Province, China

Funding: This study was supported by the National Natural Science Foundation of China, No. 81201546 (to YXL); the Doctoral Start-up Program of Natural Science Foundation of Guangdong Province of China, No. 2017A030310302 (to ZWZ); the Medical Scientific Research Foundation of Guangdong Province of China, No. A2016018 (to BH); the Science and Technology Project of Guangdong Province of China, No. 2016A010103012 (to JHL).

Graphical Abstract



*Correspondence to:

Zhao-Wei Zhu, MD, PhD,

nmtmemoir@aliyun.com;

Bo He, MD, PhD,

hebodoc@gmail.com.

#These authors contributed equally to this paper.

orcid:

0000-0003-4469-5417

(Zhao-Wei Zhu)

0000-0002-9690-4527

(Bo He)

doi: 10.4103/1673-5374.241469

Received: 2018-07-05

Accepted: 2018-08-20

Abstract

An aging-induced decrease in Schwann cell viability can affect regeneration following peripheral nerve injury in mammals. It is therefore necessary to investigate possible age-related changes in gene expression that may affect the biological function of peripheral nerves. Ten 1-week-old and ten 12-month-old healthy male Sprague-Dawley rats were divided into young (1 week old) and adult (12 months old) groups according to their ages. mRNA expression in the sciatic nerve was compared between young and adult rats using next-generation sequencing (NGS) and bioinformatics ($n = 4/\text{group}$). The 18 groups of differentially expressed mRNA (DEmRNAs) were also tested by quantitative reverse transcription polymerase chain reaction ($n = 6/\text{group}$). Results revealed that (1) compared with young rats, adult rats had 3608 groups of DEmRNAs. Of these, 2684 were groups of upregulated genes, and 924 were groups of downregulated genes. Their functions mainly involved cell viability, proliferation, differentiation, regeneration, and myelination. (2) The gene with the most obvious increase of all DEmRNAs in adult rats was *Thrsp* ($\log_2\text{FC} = 9.01$, $P < 0.05$), and the gene with the most obvious reduction was *Col2a1* ($\log_2\text{FC} = -8.89$, $P < 0.05$). (3) Gene Ontology analysis showed that DEmRNAs were mainly concentrated in oligosaccharide binding, nucleotide-binding oligomerization domain containing one signaling pathway, and peptide-transporting ATPase activity. (4) Analysis using the Kyoto Encyclopedia of Genes and Genomes showed that, with increased age, DEmRNAs were mainly enriched in steroid biosynthesis, *Staphylococcus aureus* infection, and graft-versus-host disease. (5) Spearman's correlation coefficient method for evaluating NGS accuracy showed that the NGS results and quantitative reverse transcription polymerase chain reaction results were positively correlated ($r_s = 0.74$, $P < 0.05$). These findings confirm a difference in sciatic nerve gene expression between adult and young rats, suggesting that, in peripheral nerves, cells and the microenvironment change with age, thus influencing the function and repair of peripheral nerves.

Key Words: peripheral nerve injury; aging; Sprague-Dawley rat; transcriptome; sequencing; mRNA; rat age; Schwann cells; neural regeneration

Introduction

The treatment of limb paralysis and dysfunction caused by peripheral nerve injury is a major challenge in medical science. In the USA alone, the number of peripheral nerve injury surgeries performed each year has reached 50,000 cases, and the economic burden is over 7 billion US dollars. Therefore, the question of how to improve treatment and effectively repair peripheral nerve injury has become a major public health issue that needs to be addressed by the global healthcare community (Wang et al., 2010; Yang et al., 2011; Chen et al., 2018). Thus, studies of peripheral nerve regeneration have significance in both scientific research and clinical practice (Zheng et al., 2014; He et al., 2015; Hung et al., 2015; Qiu et al., 2015; Pan et al., 2017; Zou et al., 2018).

The reduction in nerve repair ability in older animals is a research hotspot in the field of peripheral nerve injury repair (Verdu et al., 2000; Amer et al., 2014). For a long time, the majority of researchers have considered that a decline in neuronal regeneration ability is the major reason that axonal regeneration is slow in old animals (Graciarena et al., 2014; Moldovan et al., 2016; Lim et al., 2017). For example, Zou et al. (2013) showed that intrinsic changes in older neurons influence neuronal regeneration ability in a *Caenorhabditis elegans* model. They found that in older neurons, let-7 down-regulating LIN-41, which contributes to a developmental decline in axonal regeneration. However, in the younger neurons, LIN-41 inhibits let-7 expression *via* Argonaute ALG-1 to ensure that axonal regeneration could only be inhibited in older neurons. Some other scholars focused on cells other than neurons. For example, Painter et al. (2014) demonstrated that the peripheral nerve regeneration ability of 24-month-old mice is worse than that of 2-month-old mice; although *in vitro* gene detection revealed that only 14 genes in the dorsal root ganglion cells of old mice are significantly different from those in young mice. In addition, genes that are directly associated with regeneration ability (such as ATF3, GAP and prr1a) did not markedly differ between old and young mice. Therefore, some researchers have suggested that the major factor influencing peripheral nerve regeneration in mammals such as mice, rats, and humans is not the neurons themselves, but instead the decline of Schwann cell viability in peripheral nerves (Michio et al., 2014; Couve et al., 2017; Xu et al., 2017).

This study therefore aimed to compare mRNA expression in the sciatic nerves of Sprague-Dawley rats at different ages using next-generation, high-throughput whole RNA sequencing and bioinformatics. Using these techniques, the aim was to discover age-related molecules that influence the biological functions of peripheral nerves, and to investigate any underlying mechanisms, to provide theoretical bases for improving the treatment of aging peripheral nerves after injury (Canta et al., 2016; Sakita et al., 2016; Zhou. et al., 2017).

Materials and Methods

Animals

Ten 1-week-old and ten 12-month-old healthy male Sprague-Dawley rats, bought from the Animal Center of

Medical School of Sun Yat-Sen University of China, were randomly selected as experimental animals. This study was approved by the Experimental Animal Administration Committee of Sun Yat-Sen University (approval number: [2013]A-055). Efforts were taken to minimize animal suffering during the experiment.

Collection of sciatic nerves

Four rats in the young or adult group were randomly selected for the next-generation RNA high-throughput sequencing detection of sciatic nerves. Rats in the adult group were deeply anesthetized using an intraperitoneal injection of 10% chloral hydrate (Sinopharm Chemical Reagent Co., Ltd., Shanghai, China; 0.3 mL/100 g body weight). Rats in the young group were sacrificed by cervical dislocation. The specific operational procedures have been previously published (Zhu et al., 2015, 2017). Under aseptic conditions, the skin of the left leg was cut parallel to the femur, and the sciatic nerve was exposed by splitting the superficial gluteus muscle. The bilateral sciatic nerves (≥ 15 mm in length) were excised from the lower edge of piriform muscle from the rats and then external fat and connective tissue were removed.

Library preparation and RNA sequencing

Comparison of the senescence pathway genes was performed by next-generation sequencing (NGS). All sequencing programs were performed by Shanghai Biotechnology Corporation (Shanghai, China). Briefly, RNA extraction was performed using the mir Vana™ miRNA isolation kit (Cat# AM1561, Ambion, Austin, TX, USA) following the standard operating procedures provided by the manufacturer. The quality of the extracted RNA was detected using an Agilent Bioanalyzer 2100 (Agilent Technologies, Santa Clara, CA, USA). Total RNA was then purified using the RNAClean XP kit (Cat A63987, Beckman Coulter, Inc., CA, USA) and the RNase-Free DNase Set (Cat#79254, Qiagen, Germany). The quality of the initial total RNA sample for the sequencing experiment was detected using a NanoDrop ND-2000 spectrophotometer and an Agilent Bioanalyzer 2100. Total RNA that passed the quality control was used in subsequent sequencing experiments (Pertea et al., 2015).

For transcriptome sequencing, we used the number of reads mapping to the gene region to estimate the gene expression level (Pertea et al., 2016). However, in addition to being proportional to the gene expression level, the number of reads was also associated with the length of genes and the sequencing data volume. To compare gene expression levels between different genes and different samples, reads were converted into fragments per kilobase of exon model per million mapped reads (FPKM) for normalization of gene expression levels (Mortazavi et al., 2008; Yu et al., 2017). First, the number of fragments of each gene after Hisat2 comparison was counted using Stringtie v1.3.0 (The Center for Computational Biology at Johns Hopkins University, Baltimore, MD, USA). Next, normalization was performed using the trimmed mean of M values method (Robinson et al., 2010). Finally, the FPKM value of each gene was calculated using the Perl program.

Quantitative real time polymerase chain reaction (RT-PCR)

Quantitative analysis of targeted mRNA expression was performed using RT-PCR and the relative standard curve method. Six rats in each group were randomly selected. The bilateral sciatic nerves were collected using the previously described method, and total RNA was extracted. The RNA concentration and purity were detected using a Nanodrop 2000. RNA samples with high concentrations were diluted to a final concentration of 200 ng/μL. RNA (1 μg) was used for RNA reverse transcription using the RevertAid first strand cDNA synthesis kit (Thermo Fisher, Waltham, MA, USA). An appropriate amount of cDNA was amplified using FastStart Universal SYBR Green Master Mix (Roche, Basel, Switzerland) in a fluorescence quantitative PCR machine (Stepone Plus, Thermo Fisher). The specific procedures were performed according to the manufacturer's product manual. Each sample was run in triplicate. GAPDH expression was used to normalize mRNA expression. Gene information and primers are shown in **Table 1**. The specificity of RT-PCR was confirmed *via* routine agarose gel electrophoresis and melting curve analysis. The $2^{-\Delta\Delta C_t}$ method was used to calculate relative gene expression (Huang et al., 2017).

Bioinformatics and statistical analyses

Analyses of differential genes among samples were performed using edgeR (Robinson et al., 2010). After the *P*-value was obtained, multiple testing was performed for correction. The threshold value of the *P*-value was determined by controlling for false discovery rate (Benjamini et al., 1995, 2001). The corrected *P*-value was the *Q*-value. In addition, the differential expression fold was calculated based on the FPKM value, which was the fold change. The screening condition of differential genes was limited to *Q*-value ≤ 0.05 and fold change ≥ 2. Both gene ontology (GO) analysis (<http://www.geneontology.org>) and Kyoto Encyclopedia of Genes and Genomes (KEGG) pathway analysis (<http://www.genome.jp/kegg/>) were performed to determine the roles of the differentially expressed mRNAs. Fisher's exact test was used to test the significance of GO terms and pathway identifiers enriched in the differentially expressed gene list. RNA sequencing and bioinformatics analyses were performed by Shanghai Biotechnology Corporation (Shanghai, China).

The gene data of RT-PCR conform to normal distribution and were presented as the mean ± SD. SPSS 13.0 software (SPSS, Chicago, IL, USA) was used to analyze the accuracy of NGS. Quantitative RT-PCR results were compared with sequencing results using Spearman's correlation coefficient method. *P* < 0.05 was considered statistically significant.

Results

Analyses of mRNA expression levels in the sciatic nerve of young and adult rats

Transcriptome gene expression of sciatic nerves in young and adult rats was analyzed using NGS. A scatter map and a heat map were used to present the distribution of differentially expressed mRNAs (DEmRNAs; **Figure 1**). A total of

Table 1 Primer information for the genes that were detected

Gene name	Sequence (5'-3')	Product size (bp)
GAPDH	Forward: TTC CTA CCC CCA ATG TAT CCG	281
	Reverse: CAT GAG GTC CAC CAC CCT GTT	
BTC	Forward: CCT TGT CCT GGG TCT TGT GAT T	228
	Reverse: ATG CAG GAG GGA GTT TGT TCG	
NCMAP	Forward: CCG TCT TCT CGC TGA ACA TGA	149
	Reverse: CCT GGT CCT CAT TCT CCT GTT G	
ACVR1C	Forward: TTG CGG CAG GAC TGA AGT GT	240
	Reverse: CTG TGG GAA GGT GCA GAG TGA T	
DLG2	Forward: ATG ATC ATT CCT TAC CTC GGC TA	158
	Reverse: GTT GAC AAT TAT AGG AGC AGG GC	
JUN	Forward: CTT CTA CGA CGA TGC CCT CAA C	257
	Reverse: GGG TCG GTG TAG TGG TGA TGT G	
NGFR	Forward: CCT TGT GGC CTA TAT TGC TTT CA	178
	Reverse: AGG CAG TCT GCG TAT GGG TCT	
MBP	Forward: GCT TCT TTA GCG GTG ACA GGG	133
	Reverse: TGT GAG TCC TTG TAC ATG TGG CA	
PBK	Forward: GGA ATC AGT AAT TTC AAG ACG CC	169
	Reverse: AAT GGG ACA ACC CTC TCG GA	
BIRC5	Forward: CAG TCA AGA AGC AGG TGG AAG AA	123
	Reverse: TCC GGG TCT CCT CGA ACT CTT	
EGR2	Forward: GCC AAG GCC GTA GAC AAA ATC	216
	Reverse: ATA TGG GAG ATC CAA GGG CCT	
CDC20	Forward: CCC TGC AGA CAT TCA CTC AAC AT	276
	Reverse: TGT GAC CTT TGA GCT CTG CCA	
KIF2C	Forward: GCA CGG TGA ACT TGG AGA AAT C	253
	Reverse: GTG GAT ATG CGA GTG GAA CGA C	
PMP22	Forward: TCG CGG TGC TAG TGT TGC TC	151
	Reverse: TGA AGC CAT TCG CTC ACA GAT	
MAP3K	Forward: ATC CAG TTC AGC AGG TCA GGC	150
	Reverse: TTC CTC AAA CGG CAC TTC CC	
PDGFB	Forward: GAG CAT CGA GCC AAG ACA CCT	109
	Reverse: CCT TCT TGT CAT GGG TGT GCT T	
MPZ	Forward: GCT GCC CTG CTC TTC TCT TCT T	218
	Reverse: GGT TGA CCC TTG GCA TAG TGG A	
MAL	Forward: CAG TGG CTT CTC CGT CTT CGT	182
	Reverse: TGT ACA TGA CCA TCA GGG AAG TG	
WWC1	Forward: TGA GGA TGC TGG AGA AGA GGG T	196
	Reverse: GCA GAG AGA GCT GGG ATG TTC AT	

GAPDH: Glyceraldehyde 3-phosphate dehydrogenase; BTC: betacellulin; NCMAP: noncompact myelin associated protein; ACVR1C: activin A receptor type 1C; DLG2: disks large homolog 2 (DLG2); JUN: Jun proto-oncogene; AP-1: transcription factor subunit; NGFR: nerve growth factor receptor; MBP: myelin basic protein; PBK: PDZ binding kinase; BIRC5: baculoviral IAP repeat containing 5; EGR2: early growth response 2; CDC20: cell division cycle 20; KIF2C: kinesin family member 2C; PMP22: peripheral myelin protein 22; MAP3K: mitogen-activated protein kinase kinase; PDGFB: platelet derived growth factor subunit B; MPZ: myelin protein zero; MAL: myelin and lymphocyte protein; WWC1: WW and C2 domain containing 1.

30,957 mRNA groups were detected using RNA sequencing (RNA-seq), and the DEmRNA screening was performed using fold change ≥ 2.0 and *P* < 0.05 as the criteria. Compared with young rats, adult rats had 3608 groups of DEmRNAs. Of these, 2684 groups were upregulated genes, and 924 groups were downregulated genes. The gene with the greatest mRNA increase in adult rats was Thrsp ($\log_2FC = 9.01$, *P* < 0.05), and the gene with the greatest reduction was

Col2a1 ($\log_2FC = -8.89$, $P < 0.05$). The 10 groups of genes with the most obvious DE mRNAs are shown in **Table 2**. Additionally, 208 mRNAs were only expressed in adult rats and 50 mRNAs were only expressed in young rats. The gene with the greatest mRNA increase in adult rats was *Rn60_*

X_0752.3 (FPKM = 227.23, $P < 0.05$), and the gene with the most obvious increase in young rats was *Ddx3y* (FPKM = 32.69, $P < 0.05$). The top 10 most highly expressed mRNAs which were not expressed by rats in the opposite group are shown in **Table 3**.

Table 2 Top 10 mRNA groups that were only expressed in the sciatic nerve of rats in young (1 week old, $n = 4$) and adult (12 months old, $n = 4$) Sprague-Dawley rats

Dysregulation	Gene name	1-week FPKM	12-month FPKM	\log_2FC	Q value
Up	Thrsp	0.127743	65.82397	9.009228	7.57E-77
	Fcgr2b	0.180183	59.44108	8.365856	2.13E-113
	Myoc	0.961192	276.8655	8.170145	3.00E-133
	C6	0.052442	14.7549	8.13625	1.96E-57
	LOC100910255	0.074305	20.26099	8.091031	1.01E-105
	Lamb3	0.019016	5.003392	8.039568	1.26E-36
	Shh	0.229436	53.69166	7.87046	4.88E-78
	Tshr	0.029869	5.522935	7.530649	1.31E-44
	Fmo2	0.529976	77.65057	7.194926	3.16E-97
	Ces1d	0.671107	81.78231	6.929103	3.01E-95
Down	Col2a1	456.1821	0.960973	-8.8909	6.19E-186
	Agtr2	4.569736	0.056959	-6.32604	7.48E-32
	Dlk1	25.55449	0.320356	-6.31776	1.32E-69
	Marveld3	6.536042	0.095418	-6.09801	1.62E-36
	St8sia2	10.80214	0.214507	-5.65415	4.34E-29
	Epyc	30.9444	0.663528	-5.54338	2.32E-73
	Trpm5	0.952308	0.024164	-5.30051	1.67E-09
	Nrk	3.624036	0.096052	-5.23763	4.87E-32
	Igf2bp3	2.447324	0.068635	-5.15611	1.53E-16
	Alox15	40.36502	1.137897	-5.14866	3.56E-69

FPKM: Fragments Per Kilobase of exon model per Million mapped reads; FC: fold change.

Table 3 Top 10 differentially expressed mRNA groups in sciatic nerves that were upregulated or downregulated in young (1 week old, $n = 4$) and adult (12 months old, $n = 4$) Sprague-Dawley rats

Dysregulation	Gene name	FPKM		\log_2FC	Q value
		1-week FPKM	12-month FPKM		
Up	Thrsp	0.127743	65.82397	9.009228	7.57E-77
	Fcgr2b	0.180183	59.44108	8.365856	2.13E-113
	Myoc	0.961192	276.8655	8.170145	3.00E-133
	C6	0.052442	14.7549	8.13625	1.96E-57
	LOC100910255	0.074305	20.26099	8.091031	1.01E-105
	Lamb3	0.019016	5.003392	8.039568	1.26E-36
	Shh	0.229436	53.69166	7.87046	4.88E-78
	Tshr	0.029869	5.522935	7.530649	1.31E-44
	Fmo2	0.529976	77.65057	7.194926	3.16E-97
	Ces1d	0.671107	81.78231	6.929103	3.01E-95
Down	Col2a1	456.1821	0.960973	-8.8909	6.19E-186
	Agtr2	4.569736	0.056959	-6.32604	7.48E-32
	Dlk1	25.55449	0.320356	-6.31776	1.32E-69
	Marveld3	6.536042	0.095418	-6.09801	1.62E-36
	St8sia2	10.80214	0.214507	-5.65415	4.34E-29
	Epyc	30.9444	0.663528	-5.54338	2.32E-73
	Trpm5	0.952308	0.024164	-5.30051	1.67E-09
	Nrk	3.624036	0.096052	-5.23763	4.87E-32
	Igf2bp3	2.447324	0.068635	-5.15611	1.53E-16
	Alox15	40.36502	1.137897	-5.14866	3.56E-69

FPKM: Fragments Per Kilobase of exon model per Million mapped reads; FC: fold change.

GO and KEGG analyses of DEMRNAs

Clustering analysis of DEMRNAs can help to identify the function of unknown transcripts, or the unknown function of known transcripts, by gathering similar expression patterns or similar genes to a class (Yao et al., 2012). Functional classification by GO is an internationally standardized classification system for gene function that offers a dynamic, updated, and controlled vocabulary, employing strictly defined concepts to comprehensively describe the properties of genes and their products in any organism. GO classification encompasses three domains, as follows: molecular function, cellular component, and biological process (Yi et al., 2006). GO analysis revealed that DEMRNAs were mainly concentrated in genes related to oligosaccharide-binding, nucleotide-binding oligomerization domain containing one (NOD1) signaling pathway, peptide-transporting ATPase activity, fibrinogen binding, and marginal zone B cell differentiation (Figure 2 and Table 4).

The pathway enrichment of DEMRNAs was analyzed using KEGG. The KEGG pathway database comprises infor-

mation about networks of molecular interactions for numerous organisms, thus permitting functional classification. In the adult rats, DEMRNAs were mainly enriched in steroid biosynthesis, *Staphylococcus aureus* infection, graft-versus-host disease, type 1 diabetes mellitus, and allograft rejection categories (Figure 3 and Table 5).

Validation of microarray sequencing accuracy using quantitative RT-PCR

Five groups of upregulated mRNAs, namely nerve growth factor receptor (*NGFR*), betacellulin (*BTC*), activin A receptor type 1C (*ACVR1C*), disks large homolog 2 (*DLG2*), and Jun proto-oncogene (*JUN*), and five groups of downregulated mRNAs, namely noncompact myelin associated protein (*NCMAP*), myelin basic protein (*MBP*), PDZ binding kinase (*PBK*), baculoviral IAP repeat containing 5 (*BIRC5*), and early growth response 2 (*EGR2*), were selected for quantitative RT-PCR analyses in rats with different genotypes. The housekeeping gene GAPDH was used as the internal control to compare the sequencing results. Among the 10 groups of

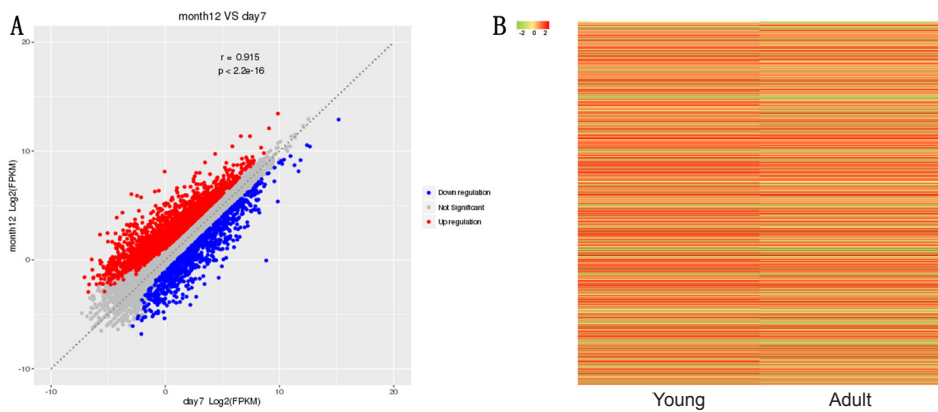


Figure 1 Scatter map and heat map of mRNA expression in the sciatic nerve in young (1 week old, $n = 4$) and adult (12 months old, $n = 4$) Sprague-Dawley rats. (A) Scatter map of mRNA expression. Red indicates upregulated genes in adult rats compared with young rats, while blue indicates downregulated genes. (B) Heat map of mRNA expression. Green in the heat map indicates a fold change ≤ 2 , and red indicates a fold change > 2 .

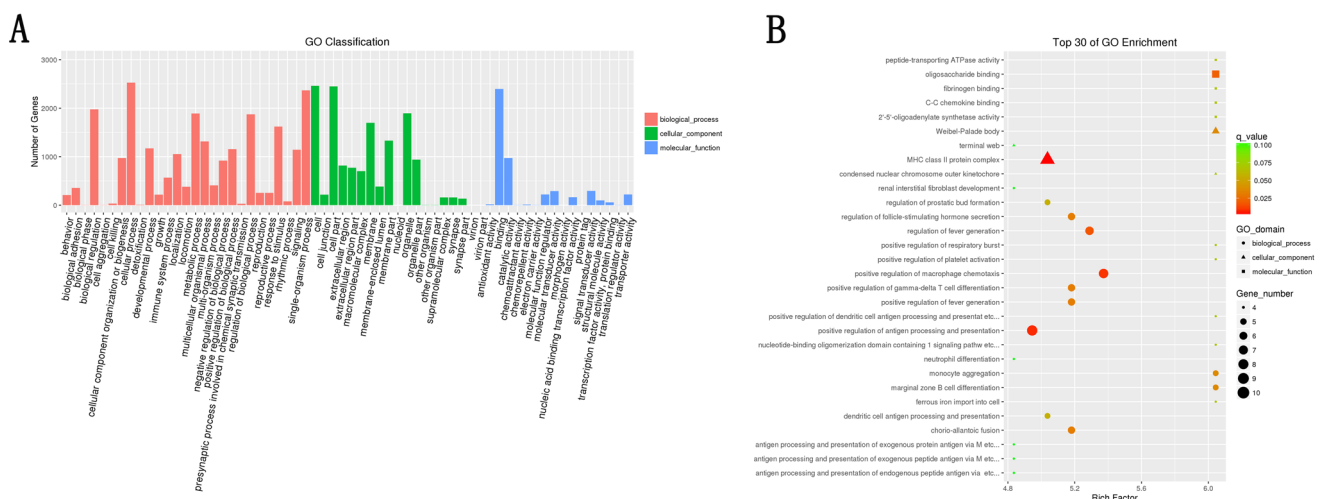


Figure 2 Schematic diagram of the Gene Ontology (GO) category and gene enrichment of differentially expressed mRNAs (DEMRNAs) in the sciatic nerve of 12-month-old and 1-week-old Sprague-Dawley rats.

(A) GO classification: Red columns represent biological process; green columns represent cellular component; blue columns represent molecular function. (B) GO enrichment: Different shapes indicate different types of function. Circles represent biological process; triangles represent cellular component, and squares represent molecular function. The area of the circles represents the number of DEMRNAs involved in the terms. Different colors indicate different Q -values of DEMRNAs in the GO terms between adult rats and young rats. Green represents $Q > 0.10$; yellow represents $Q > 0.05$ and $Q < 0.075$; orange represents $Q < 0.05$ and $Q > 0.025$; and red represents $Q < 0.025$. The standard of the test was set as 0.05 ($n = 4$ rats per group).

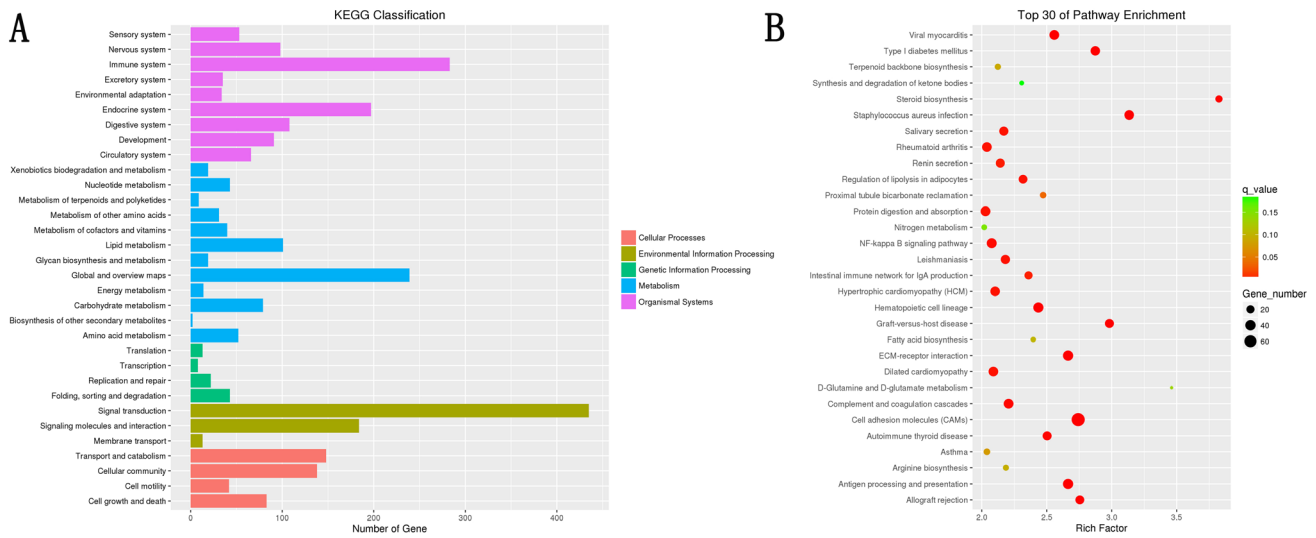


Figure 3 Schematic diagram of the pathway classification and gene enrichment of differentially expressed mRNAs (DEmRNAs) in the sciatic nerve of 12-month-old and 1-week-old Sprague Dawley rats.

(A) Kyoto Encyclopedia of Genes and Genomes (KEGG) classification: Orange columns represent cellular process; brown columns represent environmental information processing; green columns represent genetic information processing; blue columns represent metabolism; and purple columns represent organismal systems. (B) KEGG pathway enrichment: The area of the circles represents the number of DEmRNAs involved in the pathway. Different colors indicate different Q-values of DEmRNAs in the pathway between adult rats and young rats. Green represents $Q > 0.15$; yellow represents $Q > 0.10$ and $Q < 0.15$; orange represents $Q < 0.10$ and $Q > 0.05$; and red represents $Q < 0.05$. The standard of the test was set as 0.05 ($n = 4$ per group).

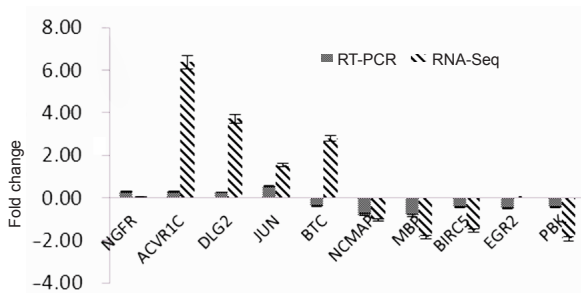


Figure 4 Comparison of quantitative RT-PCR ($n = 6$ /group) and RNA sequencing (RNA-seq; $n = 4$ /group) results of differentially expressed mRNAs in the sciatic nerve of 12-month-old and 1-week-old Sprague-Dawley rats.

To achieve baseline consistency, the quantitative RT-PCR fold change data were expressed as $2^{\Delta\Delta Ct}$, and RNA-seq data are expressed as $\log_2 FC$. NGFR: Nerve growth factor receptor; ACVR1C: activin A receptor type 1C; DLG2: discs large MAGUK scaffold protein 2; JUN: Jun proto-oncogene; BTC: betacellulin; NCMAP: noncompact myelin associated protein; MBP: myelin basic protein; BIRC5: baculoviral IAP repeat containing 5; EGR2: early growth response 2; PBK: PDZ binding kinase; FC: fold change; RT-PCR: real time polymerase chain reaction.

DEmRNAs, only BTC expression differed from the sequencing results. The sequencing results showed that BTC expression was upregulated, whereas the quantitative RT-PCR results demonstrated that BTC expression was downregulated. In contrast, the fold changes of expression in the quantitative RT-PCR results of other DEmRNAs were similar to those of the RNA microarray sequencing results (Figure 4).

A total of 18 groups of DEmRNAs were randomly selected, including the above 10 groups of genes, as well as *KIF2C*, *MAP3K*, *PDGFB*, *MPZ*, *PMP22*, *MAL*, *WWC1* and *CDC20*. To evaluate the accuracy of NGS sequencing, the correlation

between RNA sequencing results and quantitative RT-PCR results was evaluated using Spearman correlation coefficient analyses. The correlation coefficient r_s was 0.74 and $P < 0.05$, indicating that the NGS results and quantitative RT-PCR results were positively correlated (Figure 5).

Discussion

After peripheral nerve injury, neurons initiate axonal regeneration. Distal axons, cut from the neuronal cell body, develop Wallerian degeneration (Szepanowski and Kieseier, 2016; Xiao et al., 2016; Roberts et al., 2017; Cervellini et al., 2018). Proximal axons form growth cones and extend to distal ends, which grow into the target organ to achieve functional recovery (Scheib et al., 2013; Kızılay et al., 2016;

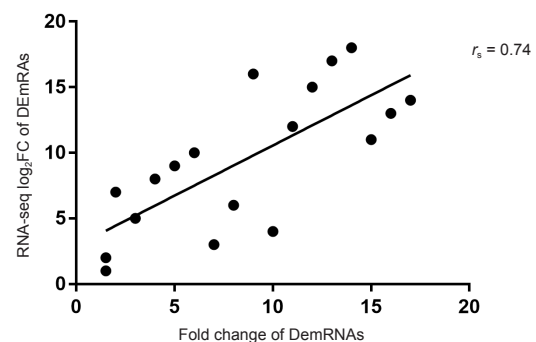


Figure 5 Scatter map of Spearman correlation coefficient analyses between quantitative real time polymerase chain reaction and sequencing data (Seq) of differentially expressed mRNAs (DEmRNAs) in the sciatic nerve of 12-month-old (adult) and 1-week-old (young) Sprague-Dawley rats. The correlation coefficient r_s was 0.74, and $P < 0.05$ ($n = 6$ /group).

Table 4 Categories in Gene Ontology (GO) analyses that corresponded to the top 20 groups of differentially expressed mRNAs (DEmRNAs) in the sciatic nerve of Sprague-Dawley rats at the ages of 1 week and 12 months

GO ID	GO term	DEmRNAs count	Enrichment factor	Q value
GO:0070492	oligosaccharide binding	6	6.044343	0.020547
GO:0070427	nucleotide-binding oligomerization domain containing 1 signaling pathway	4	6.044343	0.067853
GO:0015440	peptide-transporting ATPase activity	4	6.044343	0.067853
GO:0070051	fibrinogen binding	4	6.044343	0.067853
GO:0002315	marginal zone B cell differentiation	5	6.044343	0.037313
GO:0001730	2'-5'-oligoadenylate synthetase activity	4	6.044343	0.067853
GO:0000942	condensed nuclear chromosome outer kinetochore	4	6.044343	0.067853
GO:0033093	Weibel-Palade body	5	6.044343	0.037313
GO:0097460	ferrous iron import into cell	4	6.044343	0.067853
GO:0070487	monocyte aggregation	5	6.044343	0.037313
GO:0019957	C-C chemokine binding	4	6.044343	0.067853
GO:0002606	positive regulation of dendritic cell antigen processing and presentation	4	6.044343	0.067853
GO:0010572	positive regulation of platelet activation	4	6.044343	0.067853
GO:0060267	positive regulation of respiratory burst	4	6.044343	0.067853
GO:0010759	positive regulation of macrophage chemotaxis	8	5.372749	0.00931
GO:0031620	regulation of fever generation	7	5.2888	0.017348
GO:0060710	chorio-allantoic fusion	6	5.180865	0.031748
GO:0045588	positive regulation of gamma-delta T cell differentiation	6	5.180865	0.031748
GO:0046880	regulation of follicle-stimulating hormone secretion	6	5.180865	0.031748
GO:0031622	positive regulation of fever generation	6	5.180865	0.031748

Table 5 Pathways in the Kyoto Encyclopedia of Genes and Genomes (KEGG) analyses that corresponded to the top 20 groups of enriched differentially expressed mRNAs (DEmRNAs, age of 12 months vs. age of 1 week)

Pathway ID	Pathway description	DEmRNAscount	Enrichment factor	Q value
rno00100	Steroid biosynthesis	14	3.825181	0.000361
rno05150	Staphylococcus aureus infection	32	3.13438	4.18E-06
rno05332	Graft-versus-host disease	27	2.982246	2.82E-05
rno04940	Type I diabetes mellitus	31	2.873765	1.78E-05
rno05330	Allograft rejection	26	2.754576	0.000135
rno04514	Cell adhesion molecules (CAMs)	75	2.741893	2.41E-11
rno04512	ECM-receptor interaction	39	2.663965	8.48E-06
rno04612	Antigen processing and presentation	39	2.663965	8.48E-06
rno05416	Viral myocarditis	34	2.55804	3.73E-05
rno05320	Autoimmune thyroid disease	27	2.502956	0.000441
rno04964	Proximal tubule bicarbonate reclamation	10	2.472056	0.035383
rno04640	Hematopoietic cell lineage	38	2.435433	3.59E-05
rno04672	Intestinal immune network for IgA production	20	2.35969	0.003868
rno04923	Regulation of lipolysis in adipocytes	25	2.317552	0.001579
rno04610	Complement and coagulation cascades	34	2.20631	0.000603
rno05140	Leishmaniasis	29	2.181858	0.001555
rno04970	Salivary secretion	28	2.169506	0.001734
rno04924	Renin secretion	26	2.142448	0.003209
rno05410	Hypertrophic cardiomyopathy (HCM)	32	2.102812	0.001623
rno05414	Dilated cardiomyopathy	33	2.089189	0.00162

Ma et al., 2016; Wang et al., 2016; Tallon and Farah, 2017). However, with increasing age, the speed of nerve regeneration and functional recovery greatly decreases (Kawabuchi et al., 2011). We previously reviewed literature on the repair efficacy of peripheral nerve injury in the upper limb from a 20-year period, to perform a univariate meta-analysis. The results indicated that a 1-year increase in age had an odds ratio of 0.97–0.98 for excellent recovery (He et al., 2014). For example, if the regeneration ability following nerve injury in

a newborn is 100%, the nerve regeneration ability after injury during old age (e.g., in a 60-year-old male) is only 16–30% of that at birth. These results suggest that the “aging” factor has a relatively large influence on nerve injury repair efficacy (Esquisatto et al., 2014; Ugrenović et al., 2016; Scheib et al., 2016; Castelnovo et al., 2017).

Some researchers suggested that the major factor influencing peripheral nerve regeneration in mammals, such as mice, rats, and humans, is not neurons themselves but instead the

decline of Schwann cell viability in peripheral nerves (Belin et al., 2017; Plaza-Zabala et al., 2017). Kang et al. (2013) used phase-contrast microscopy and immunohistochemistry to detect the rate of nerve regeneration in mice at different ages. The results showed that the axonal regeneration rate of old animals does not markedly differ from that of young animals. However, endoneurial tubes in old animals have more nerve and myelin sheath debris to block the growth of axons. Therefore, these researchers considered that the “dedifferentiation-proliferation-differentiation” timing of Schwann cells, and degree of Schwann cells impact the time course of Wallerian degeneration to further influence the rate of axonal regeneration. Painter et al. (2014) compared the differences in gene expression in Schwann cells between old and young mice. They demonstrated that the expression levels of growth-factor-related coding genes (BTC, NGFR, and BDNF) and mitosis-related genes (KIF2C, PBK, BIRC5, and CDC20) markedly decrease in old mice, while expression levels of myelination-associated genes (PMP2, MPZ, MAL, and EGR2) increase in old mice. These results suggest that the dedifferentiation ability of Schwann cells declines in old mice, thereby reducing the rate of nerve regeneration.

In the current study, we compared transcriptome gene expression in the sciatic nerve of rats at different ages and found that 3608 groups of mRNAs were differentially expressed between adult rats (12 months old) and young rats (1 week old). The upregulated genes were mainly concentrated in changes in development, anatomical morphology, cell differentiation, and the extracellular matrix. To validate the accuracy of microarray sequencing, we selected 10 groups of genes associated with proliferation, differentiation, myelination, injury, and synaptic transmission for quantitative RT-PCR. The results were compared with sequencing results to validate their accuracy. The proliferation- and differentiation-related genes included NGFR, ACVR1C, BTC, survivin (BIRC5) and EGR2. The injury-related genes included JUN, and the myelination-related genes included MBP and NCMAP. The synaptic transmission-related genes included DLG2. The PCR results demonstrated that the expression trends of all groups of genes, except for BTC, were consistent with the microarray results. Spearman correlation coefficient analysis showed that the results of these two groups showed a positive correlation, which further indicated the accuracy of the microarray sequencing. The growth, development, conduction, and repair of peripheral nerves is a complex process. Although more than 1000 groups of differential mRNA sequences were obtained from the NGS array of sciatic nerves of rats at different ages, further in-depth experimental studies, as well as the function and regulatory method of deep mining of differential sequences, are required to fill the gap between age and peripheral nerve structure and function.

Collectively, this study showed that gene expression in sciatic nerves differs between adult and young rats, and these differences occur in genes involved in cell activity, proliferation, differentiation, regeneration, myelination, and injury. These results suggest that, in peripheral nerves, both cells and the microenvironment change with age to influence the function

and repair of peripheral nerves. These results thus provide important theoretical bases for further studies on the relationship between peripheral nerves, regeneration, and age.

Author contributions: Specimen harvesting, data analysis and interpretation: JHL and QT; statistical analysis: XXL, JQ and RXZ; study design, data analysis and paper editing: QT, ZWZ and BH; paper revision: BH and YBX. All authors read and approved the final manuscript.

Conflicts of interest: The authors declare that there are no conflicts of interest associated with this manuscript.

Financial support: This study was supported by the National Natural Science Foundation of China, No. 81201546 (to YXL); the Doctoral Startup Program of Natural Science Foundation of Guangdong Province of China, No. 2017A030310302 (to ZWZ); the Medical Scientific Research Foundation of Guangdong Province of China, No. A2016018 (to BH); the Science and Technology Project of Guangdong Province of China, No. 2016A010103012 (to JHL). The funding sources had no role in study conception and design, data analysis or interpretation, paper writing or deciding to submit this paper for publication.

Institutional review board statement: This study was approved by the Experimental Animal Administration Committee of Sun Yat-sen University of China (approval number: [2013]A-055). All experimental procedures described here were in accordance with the National Institutes of Health (NIH) guidelines for the Care and Use of Laboratory Animals.

Copyright license agreement: The Copyright License Agreement has been signed by all authors before publication.

Data sharing statement: Datasets analyzed during the current study are available from the corresponding author on reasonable request.

Plagiarism check: Checked twice by iThenticate.

Peer review: Externally peer reviewed.

Open access statement: This is an open access journal, and articles are distributed under the terms of the Creative Commons Attribution-NonCommercial-ShareAlike 4.0 License, which allows others to remix, tweak, and build upon the work non-commercially, as long as appropriate credit is given and the new creations are licensed under the identical terms.

Open peer reviewers: Ben Christensen, University of Utah, Salt Lake City, USA; Dumitru Andrei Iacobas, Prairie View A&M University, USA.

Additional file: Open peer review reports 1 and 2.

References

- Amer MG, Mazen NF, Mohamed NM (2014) Role of calorie restriction in alleviation of age-related morphological and biochemical changes in sciatic nerve. *Tissue Cell* 46:497-504.
- Belin S, Zuloaga KL, Poitelon Y (2017) Influence of mechanical stimuli on Schwann Cell Biology. *Front Cell Neurosci* 11:347.
- Benjamini Y, Hochberg Y (1995) Controlling the false discovery rate: a practical and powerful approach to multiple testing. *J Roy Statist Soc Ser B* 57:289-300.
- Benjamini Y, Yekutieli D (2001) The control of the false discovery rate in multiple testing under dependency. *Ann Statist* 29:1165-1188.
- Canta A, Chiorazzi A, Carozzi VA, Meregalli C, Oggioni N, Bossi M, Rodriguez-Menendez V, Avezza F, Crippa L, Lombardi R, de Vito G, Piazza V, Cavaletti G, Marmiroli P (2016) Age-related changes in the function and structure of the peripheral sensory pathway in mice. *Neurobiol Aging* 45:136-148.
- Castelnovo LF, Bonalume V, Melfi S, Ballabio M, Colleoni D, Magnaghi V (2017) Schwann cell development, maturation and regeneration: a focus on classic and emerging intracellular signaling pathways. *Neural Regen Res* 12:1013-1023.
- Cervellini I, Galino J, Zhu N, Allen S, Birchmeier C, Bennett DL (2018) Sustained MAPK/ERK activation in adult Schwann cells impairs nerve repair. *J Neurosci* 38:679-690.
- Chen H, Xiang J, Wu J, He B, Lin T, Zhu Q, Liu X, Zheng C (2018) Expression patterns and role of PTEN in rat peripheral nerve development and injury. *Neurosci Lett* 676:78-84.
- Couve E, Lovera M, Suzuki K, Schmachtenberg O (2017) Schwann cell phenotype changes in aging human dental pulp. *J Dent Res* 97:347-355.
- Esquisatto MAM, de Aro AA, Fêo HB, Gomes L (2014) Changes in the connective tissue sheath of Wistar rat nerve with aging. *Ann Anat* 196:441-448.

- Graciarena M, Dambly-Chaudière C, Ghysen A (2014) Dynamics of axonal regeneration in adult and aging zebrafish reveal the promoting effect of a first lesion. *Proc Natl Acad Sci U S A* 111:1610-1615.
- He B, Zhu Q, Chai Y, Ding X, Tang J, Gu L, Xiang J, Yang Y, Zhu J, Liu X (2015) Safety and efficacy evaluation of a human acellular nerve graft as a digital nerve scaffold: a prospective, multicentre controlled clinical trial. *J Tissue Eng Regen Med* 9:286-295.
- He B, Zhu Z, Zhu Q, Zhou X, Zheng C, Li P, Zhu S, Liu X, Zhu J (2014) Factors predicting sensory and motor recovery after the repair of upper limb peripheral nerve injuries. *Neural Regen Res* 9:661-672.
- Huang G, Kang Y, Huang Z, Zhang Z, Meng F, Chen W, Fu M, Liao W, Zhang Z (2017) Identification and characterization of long non-coding RNAs in osteogenic differentiation of human adipose-derived stem cells. *Cell Physiol Biochem* 42:1037-1050.
- Hung HA, Sun G, Keles S, Svaren J (2015) Dynamic regulation of Schwann cell enhancers after peripheral nerve injury. *J Biol Chem* 290:6937-6950.
- Kang H, Lichtman JW (2013) Motor axon regeneration and muscle reinnervation in young adult and aged animals. *J Neurosci* 33:19480-19491.
- Kawabuchi M, Tan H, Wang S (2011) Age affects reciprocal cellular interactions in neuromuscular synapses following peripheral nerve injury. *Ageing Res Rev* 10:43-53.
- Kızılay Z, Erken HA, Çetin NK, Aktaş S, Abas Bİ, Yılmaz A (2016) Boric acid reduces axonal and myelin damage in experimental sciatic nerve injury. *Neural Regen Res* 11:1660-1665.
- Lim EF, Musa A, Frederick A, Ousman SS (2017) AlphaB-crystallin expression correlates with aging deficits in the peripheral nervous system. *Neurobiol Aging* 53:138-149.
- Ma KH, Hung HA, Svaren J (2016) Epigenomic regulation of Schwann cell reprogramming in peripheral nerve injury. *J Neurosci* 36:9135-9147.
- Moldovan M, Rosberg MR, Alvarez S, Klein D, Martini R, Krarup C (2016) Aging-associated changes in motor axon voltage-gated Na⁺ channel function in mice. *Neurobiol Aging* 39:128-139.
- Mortazavi A, Williams BA, McCue K, Schaeffer L, Wold B (2008) Mapping and quantifying mammalian transcriptomes by RNA-Seq. *Nat Methods* 5:621-628.
- Painter MW, Brosius Lutz A, Cheng YC, Latremoliere A, Duong K, Miller CM, Posada S, Cobos EJ, Zhang AX, Wagers AJ, Havton LA, Barres B, Omura T, Woolf CJ (2014) Diminished Schwann cell repair responses underlie age-associated impaired axonal regeneration. *Neuron* 83:331-343.
- Pan B, Zhou HX, Liu Y, Yan JY, Wang Y, Yao X, Deng YQ, Chen SY, Lu L, Wei ZJ, Kong XH, Feng SQ (2017) Time-dependent differential expression of long non-coding RNAs following peripheral nerve injury. *Int J Mol Med* 39:1381-1392.
- Pertea M, Pertea GM, Antonescu CM, Chang TC, Mendell JT, Salzberg SL (2015) StringTie enables improved reconstruction of a transcriptome from RNA-seq reads. *Nat Biotechnol* 33:290-295.
- Pertea M, Kim D, Pertea GM, Leek JT, Salzberg SL (2016) Transcript-level expression analysis of RNA-seq experiments with HISAT, stringtie and ballgown. *Nat Protoc* 11:1650-1667.
- Plaza-Zabala A, Sierra-Torre V, Sierra A (2017) Autophagy and microglia: novel partners in neurodegeneration and aging. *Int J Mol Sci* 18:598.
- Qiu L, He B, Hu J, Zhu Z, Liu X, Zhu J (2015) Cartilage oligomeric matrix protein angiopoietin-1 provides benefits during nerve regeneration in vivo and in vitro. *Ann Biomed Eng* 43:2924-2940.
- Roberts SL, Dun X, Doddrell RDS, Mindos T, Drake LK, Onaitis MW, Florio F, Quattrini A, Lloyd AC, D'Antonio M, Parkinson DB (2017) Sox2 expression in Schwann cells inhibits myelination in vivo and induces influx of macrophages to the nerve. *Development* 144:3114-3125.
- Robinson MD, Oshlack A (2010) A scaling normalization method for differential expression analysis of RNA-seq data. *Genome Biol* 11:R25.
- Robinson MD, McCarthy DJ, Smyth GK (2010) EdgeR: a Bioconductor package for differential expression analysis of digital gene expression data. *Bioinformatics* 26:139-140.
- Sakita M, Murakami S, Fujino H (2016) Age-related morphological regression of myelinated fibers and capillary architecture of distal peripheral nerves in rats. *BMC Neurosci* 17:39.
- Scheib J, Hoke A (2013) Advances in peripheral nerve regeneration. *Nat Rev Neurol* 9:668-676.
- Scheib JL, Hoke A (2016) An attenuated immune response by Schwann cells and macrophages inhibits nerve regeneration in aged rats. *Neurobiol Aging* 45:1-9.
- Szeponowski F, Kieseier BC (2016) Targeting lysophospholipid signaling as a therapeutic approach towards improved peripheral nerve regeneration. *Neural Regen Res* 11:1754-1755.
- Tallon C, Farah MH (2017) Beta secretase activity in peripheral nerve regeneration. *Neural Regen Res* 12:1565-1574.
- Ugrenović S, Jovanović I, Vasović L, Kundalić B, Čukuranović R, Stefanović V (2016) Morphometric analysis of the diameter and g-ratio of the myelinated nerve fibers of the human sciatic nerve during the aging process. *Anat Sci Int* 91:238-245.
- Verdu E, Ceballos D, Vilches JJ, Navarro X (2000) Influence of aging on peripheral nerve function and regeneration. *J Peripher Nerv Syst* 5:191-208.
- Wang D, Liu X, Zhu J, Hu J, Jiang L, Zhang Y, Yang L, Wang H, Zhu Q, Yi J, Xi T (2010) Repairing large radial nerve defects by acellular nerve allografts seeded with autologous bone marrow stromal cells in a monkey model. *J Neurotraum* 27:1935-1943.
- Wang Y, Zhao Y, Sun C, Hu W, Zhao J, Li G, Zhang L, Liu M, Liu Y, Ding F, Yang Y, Gu X (2016) Chitosan degradation products promote nerve regeneration by stimulating Schwann cell proliferation via miR-27a/FOXO1 axis. *Mol Neurobiol* 53:28-39.
- Xiao B, Rao F, Guo ZY, Sun X, Wang YG, Liu SY, Wang AY, Guo QY, Meng HY, Zhao Q, Peng J, Wang Y, Lu SB (2016) Extracellular matrix from human umbilical cord-derived mesenchymal stem cells as a scaffold for peripheral nerve regeneration. *Neural Regen Res* 11:1172-1179.
- Xu S, Ao J, Gu H, Wang X, Xie C, Meng D, Wang L, Liu M (2017) IL-22 impedes the proliferation of schwann cells: transcriptome sequencing and bioinformatics analysis. *Mol Neurobiol* 54:2395-2405.
- Yang LM, Liu XL, Zhu QT, Zhang Y, Xi TF, Hu J, He CF, Jiang L (2011) Human peripheral nerve-derived scaffold for tissue-engineered nerve grafts: histology and biocompatibility analysis. *J Biomed Mater Res B Appl Biomater* 96:25-33.
- Yao D, Li M, Shen D, Ding F, Lu S, Zhao Q, Gu X (2012) Gene expression profiling of the rat sciatic nerve in early Wallerian degeneration after injury. *Neural Regen Res* 7:1285-1292.
- Yi M, Horton JD, Cohen JC, Hobbs HH, Stephens RM (2006) Whole pathway scope: a comprehensive pathway-based analysis tool for high-throughput data. *BMC Bioinformatics* 7:30.
- Yu D, Du Z, Pian L, Li T, Wen X, Li W, Kim S, Xiao J, Cohen P, Cui J, Hoffman AR, Hu J (2017) Mitochondrial DNA hypomethylation is a biomarker associated with induced senescence in human fetal heart mesenchymal stem cells. *Stem Cells Int* 2017:1-12.
- Zheng C, Zhu Q, Liu X, Huang X, He C, Jiang L, Quan D (2014) Improved peripheral nerve regeneration using acellular nerve allografts loaded with platelet-rich plasma. *Tissue Eng Part A* 20:3228-3240.
- Zhou J, Fan Y, Chen H (2017) Analyses of long non-coding RNA and mRNA profiles in the spinal cord of rats using RNA sequencing during the progression of neuropathic pain in an SNI model. *RNA Biol* 14:1810-1826.
- Zhu Z, Huang Y, Zou X, Zheng C, Liu J, Qiu L, He B, Zhu Q, Liu X (2017) The vascularization pattern of acellular nerve allografts after nerve repair in Sprague-Dawley rats. *Neurol Res* 39:1014-1021.
- Zhu Z, Zhou X, He B, Dai T, Zheng C, Yang C, Zhu S, Zhu J, Zhu Q, Liu X (2015) Ginkgo biloba extract (EGb 761) promotes peripheral nerve regeneration and neovascularization after acellular nerve allografts in a rat model. *Cell Mol Neurobiol* 35:273-282.
- Zou J, Liu S, Sun J, Yang W, Xu Y, Rao Z, Jiang B, Zhu Q, Liu X, Wu J, Chang C, Mao H, Ling E, Quan D, Zeng Y (2018) Peripheral nerve-derived matrix hydrogel promotes remyelination and inhibits synapse formation. *Adv Funct Mater* 28:1705739.
- Zou Y, Chiu H, Zinovyeva A, Ambros V, Chuang CF, Chang C (2013) Developmental decline in neuronal regeneration by the progressive change of two intrinsic timers. *Science* 340:372-376.

P-Reviewer: Christensen B, Iacobas DA; C-Editor: Zhao M; S-Editor: Wang J, Li CH; L-Editor: Qiu Y, Song LP; T-Editor: Liu XL